

## **Section 8**

**Development of and advances in  
ocean modelling and data  
assimilation, sea-ice modelling, wave  
modelling**



# Simulation of Cold pool and its interannual variability in the tropical Indian Ocean

D. W. Ganer and A. A. Deo

E- mail : [tsd@tropmet.res.in](mailto:tsd@tropmet.res.in)

Indian Institute of Tropical Meteorology, Pune -411008

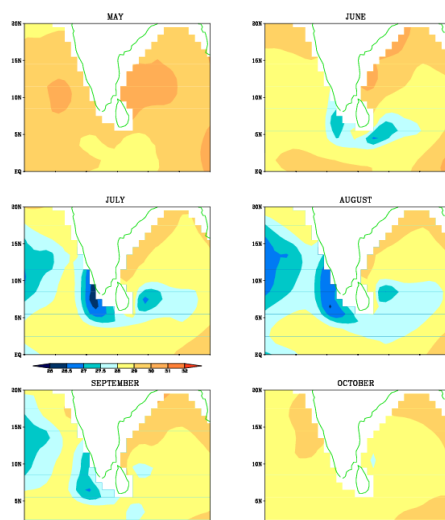
Annual cycle of sea surface temperature in the Indian Ocean shows warming in the equatorial region from February. This warm belt migrates northward till May. The observations also indicate a region of cold SST from June to September at the southern tip of India which shows importance for the convective heat source during the summer monsoon.

A 2½ layer thermodynamic ocean model has been used to simulate the cold pool in the Indian Ocean. Initially the model is spun up for ten years to reach the steady state with mean surface winds and heat fluxes those are obtained by averaging the five years daily NCEP surface winds and heat fluxes over the period 2000 to 2004. Since the numerical solution reached a quasi-equilibrium state after this integration, the model solutions by the end of this integration are considered as steady state solutions for the inter-annual runs. Further the model integration is carried out for 5 years for the period 2000 to 2004 with interannually varying daily NCEP surface winds and heat fluxes from the steady state. The warm sea surface temperature appears over equatorial region from February and further migrates northward, the sea surface starts cooling at the southern tip of India from June. The mean model simulated sea surface temperature from June to September shows that there is a cold region at the southern tip of India in the small domain 70° E-95° E, 5° N-10° N, where SSTs are below 28° C (Fig. 1). We define this as a ‘cold pool’ which is also observed from OI SST V2. The model entrainment caused by the winds shows that this cold pool is a result of upwelling at the southern India and Sri Lankan coasts and the eastward advection of this upwelled cold water. Further to examine the interannual variability of this cooling, July and August months of the three years from 2002 to 2004 are considered in which the years 2002 and 2004 have deficient monsoon. The simulated cold pool (Fig. 2) shows interannual variability during the years 2002 to 2004. The results show that the areal extent of model simulated cold pool in the month of July and August during the years 2002 and 2004 is same as the domain mentioned above where as during the year 2003, it is much smaller. Such variability is compared and is in agreement with OI SST V2.

The interannual variability of convective heating is also examined by considering OLR as a proxy for convective heating. It is found that the shifting of atmospheric convection to the northeast of Bay of Bengal (Joseph et al. 2004), extent of the cold pool transport to the northern low level jet (Joseph et al. 2004), and the evolution of cold pool is observed during the evolution of cold pool in observational experiments. The interannual variability of convective heating is also examined by considering OLR as a proxy for convective heating. It is found that the shifting of atmospheric convection to the northeast of Bay of Bengal (Joseph et al. 2004), extent of the cold pool transport to the northern low level jet (Joseph et al. 2004), and the evolution of cold pool is observed during the evolution of cold pool in observational experiments.

## References :

1. Joseph P. V. and Joseph P. V. Stream of the Asian Monsoon
2. Behera S.K., P. S. and P. S. Variability in the Indian Ocean



Model SST

cross equatorial low level jet (Joseph et al. 2004) are dependent on the free due to the moisture heat flux (Behera et al. 2004). The activity and the axis of convection is shifted to the north. This may be due to the weakening of the low level jet. The phenomenon of interannual variability of the same.

of the Low-Level Jet (Joseph et al. 2004). The evolution of Interannual SST (Joseph et al. 2004).

Fig. 1 Mean model simulated cold pool in the Indian ocean

Model SST

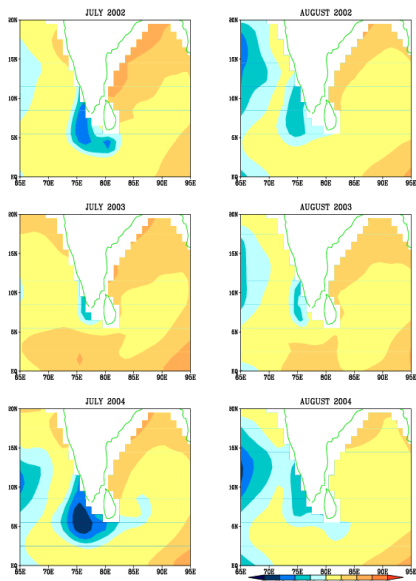


Fig. 2 Model simulated interannual variability in the cold pool

OLR (NOAA)

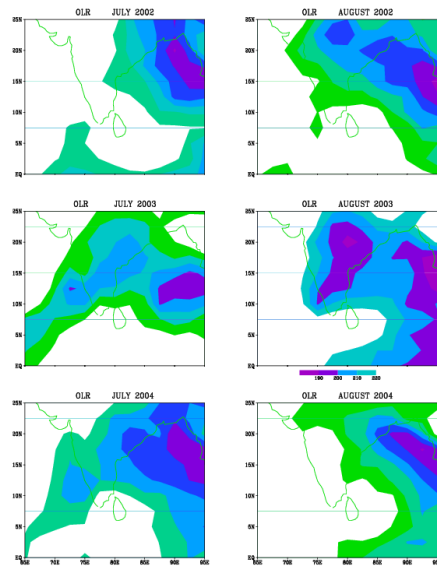


Fig. 3 Variability in Atmospheric convection in association with cold pool.

## Ensemble of Trajectories in the Southern Ocean Circulation System

Yu.D. Resnyansky, A.A. Zelenko, and B.S. Strukov

Hydrometeorological Research Center of Russian Federation,  
Bol. Predtechensky per., 11-13, 123242 Moscow, Russia E-mail: resn@mecom.ru

Long-distance transport of mass, heat and salt in the ocean is one of the primary mechanisms determining the evolution of the thermohaline structure and of climate variability. To reveal peculiar properties of mass transport and of related mixing processes in the Southern Ocean circulation system, ensemble of trajectories of liquid particles (LPs), or markers, was computed for different LPs initial positions.

Varying with time three dimensional field of ocean currents required to plot the trajectories was derived from numerical experiments with an ocean general circulation model (OGCM) based on primitive equations (Resnyansky and Zelenko, 1999; Zelenko and Resnyansky, 2007). A global OGCM version was used with computational domain over the whole World Ocean excepting part of the Arctic Basin northward of 80.3° N and with horizontal resolution 2°×2° in the Southern Ocean. The vertical structure was approximated by 32 unevenly spaced z-levels with finer resolution in the upper ocean.

The NCEP 6-hour reanalysis data on heat/fresh water fluxes and wind stress over 1979–2002 were used to specify boundary conditions at the water surface.

The ensembles were formed by a set of initial LPs positions allocated in nodes of regular 5×5×4 mesh occupying a volume  $\Delta\lambda\times\Delta\varphi\times\Delta z = 2^\circ\times 2^\circ\times 20\text{ m}$ . The area of horizontal projection of the water volume with initial markers distributed within it coincides with the size of OGCM computational cell (about 110×220 km<sup>2</sup> at  $\varphi = 60^\circ$ ). The vertical size matches the depth of the upper computational layer.

Some of the pictures illustrating the trajectories behavior are shown in Figs. 1–3. It is seen that three-dimensional time-dependent circulation in the Southern Ocean reveals the properties inherent in chaotic advection (e.g. Liu and Yang H., 1994). The trajectories become chaotic, and the LPs initially distributed within a compact volume are randomly distributed with time over vast areas (Fig. 1).

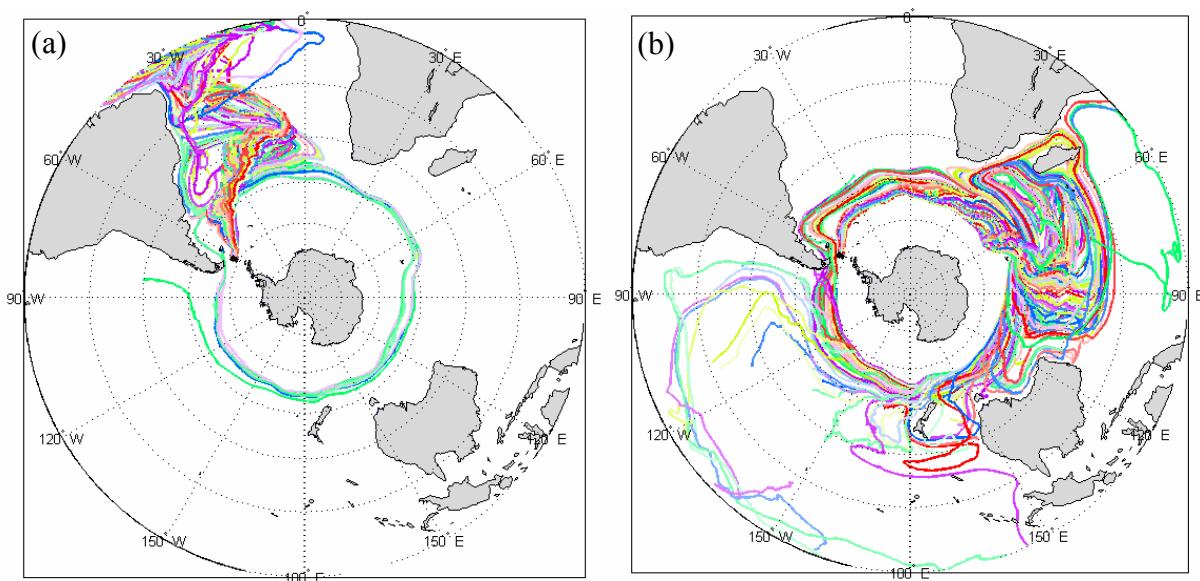


Fig. 1. Horizontal projections of LPs trajectories ensembles derived from model large scale ocean currents over 1979–2002 with starting position at different depths  $z_{p0}$  in the Drake Passage. (a) –  $z_{p0} = 10\text{ m}$ ; (b) –  $z_{p0} = 100\text{ m}$ .

The transport of LPs from the upper layer of the Southern Ocean takes place predominantly under the influence of Ekman currents. In the Southern Ocean with prevailing west winds the meridional component of Ekman currents is directed from the pole to the equator. As a consequence, all the LPs ensembles examined in the experiments traveled equatorwards, and therewith intensive mixing appeared being localized in different places depending on initial position of the control volume (Fig. 1a).

The waters from subsurface layer (from depths of an order  $z_{p0} = 100\text{ m}$ ) are to a greater extent involved into circumpolar traveling, and the mixing zones also arise in the processes (Fig. 1b). In deeper layers ( $z_{p0} \sim 1000\text{ m}$ ) the motion pattern appears as a rather tight bunch of trajectories, that is the mixing during the 24 years travel turns out here to be weak.

The ensemble mean depths  $\bar{z}_p$  of LPs being traced, as a rule, increase with time for upper starting positions and decrease for deeper ones (Fig. 2). This indicates that the chaotic transport, arising in the field of time dependent three dimensional large scale currents in the Southern Ocean, contains quite a clear evidence of an efficient mechanism of vertical mass redistribution – the net submersion of waters from upper layers and their rising from deeper layers.

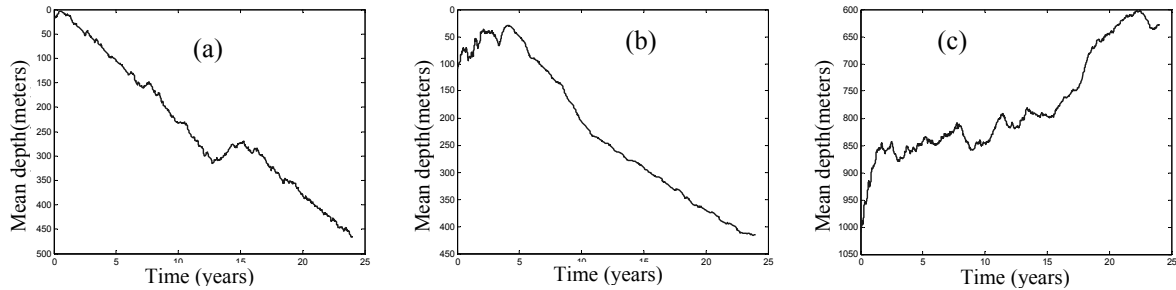


Fig. 2. Temporal changes of ensemble mean depths  $\bar{z}_p$  of LPs transported by varying with time large scale ocean currents with starting position at different depths in the Drake Passage. (a) –  $z_{p0}=10$  m; (b) –  $z_{p0}=100$  m; (c) –  $z_{p0}=1000$  m.

The vertical redistribution of markers in the system of large scale circulation can be inferred from the diagrams presented in Fig.3. Markers starting at 10 m depth are redistributed with time down to 450–500 m (Fig. 3a). The noticeable mixing occurs in the Atlantic sector (Fig. 1), to which the most part of the LPs arrives. The meridional scattering amounts here to  $45^\circ$ , that is, about 5000 km (Fig. 3a). The passages through the meridional plane from the west to the east alternate with reverse intersections. The overall pattern of motion in the neighborhood of this meridian contains all the features of pronounced mixing of the originally compact set of LPs. For the ensemble with starting position in the Drake Passage at 100 m depth the mixing encompasses the layer down to 700 m (Fig. 3b) and occurs in Indian and Pacific sectors (Fig. 1b).

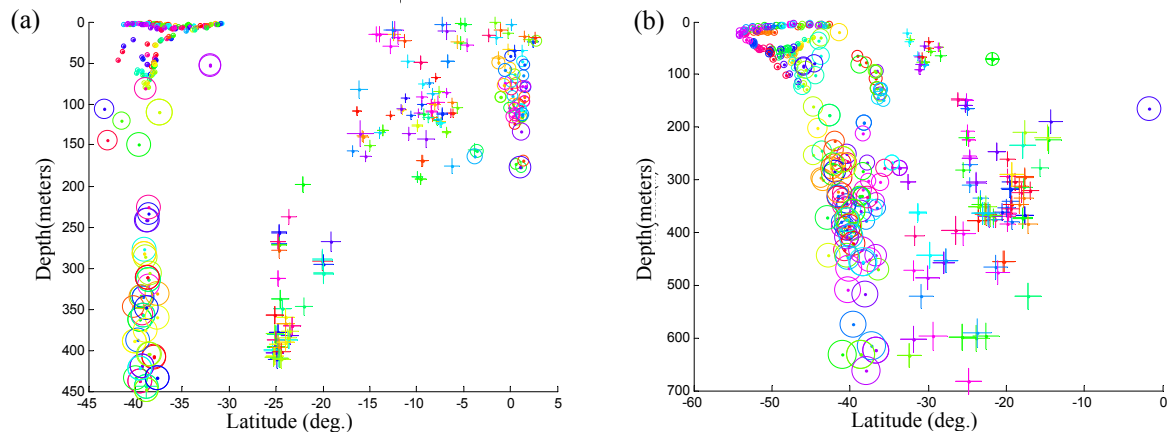


Fig. 3. Intersections of meridional planes by LPs for two starting depths in the Drake Passage. The intersections from the west to the east are marked by circles, from the east to the west – by crosses. The size of the marks is proportional to the logarithm of time elapsed from the trajectory start. Different colors correspond to individual trajectories of the ensemble. (a) –  $z_{p0}=10$  m, intersection through  $\lambda=30^\circ$  W; (b) –  $z_{p0}=100$  m, intersection through  $\lambda=60^\circ$  E.

### References

- Liu, Z., and H. Yang, 1994: The intergyre chaotic transport. *J. Phys. Oceanogr.*, **24**, 1768-1782.  
 Resnyansky, Yu.D., and A.A. Zelenko, 1999: Effects of synoptic variations of atmospheric forcing in an ocean general circulation model: Direct and indirect manifestations. *Russian Meteorology and Hydrology*, **9**, 42–50.  
 Zelenko, A.A., and Yu.D. Resnyansky, 2007: Deep convection in an ocean general circulation model: Variability at diurnal, seasonal and interannual time scales. *Okeanologiya*, **47**, 1-14.

# Improvement of multi-limit mixed-layer entrainment parameterization from the results in an ocean global circulation model

Akiyoshi Wada<sup>1\*</sup>, Hiroshi Niino<sup>2</sup>, Hideyuki Nakano<sup>1</sup>

1) Meteorological Research Institute, Tsukuba, Ibaraki, 305-0052, Japan

2) Ocean Research Institute, the University of Tokyo, Nakano, Tokyo, 164-8639, Japan

\*E-mail:awada@mri-jma.go.jp

## 1. Purpose

The purpose of this investigation is to improve a multi-limit mixed-layer entrainment parameterization (Deardorff, 1983) to improve the reproduction or prediction of oceanic impact on tropical cyclones. Even though the original parameterization, installed in a slab mixed-layer ocean model (hereafter SOM), was useful for the reproduction of sea surface cooling (SSC) by the passage of Typhoon Rex (1998) (Wada, 2005), the processes of SSC production, occurred within a mixed layer, could not be investigated by using the SOM. First, we clarify the processes of SSC production within a mixed layer from the result of numerical simulation performed using an oceanic global circulation model. Then we attempt to modify the multi-limit mixed-layer entrainment parameterization using the result of the numerical simulation.

## 2. Methods

Meteorological Research Institute Community Ocean Model (MRI.COM, Ishikawa et al, 2005) was used to perform the numerical simulation in the case of the ocean response to Rex. The MRI.COM has a horizontal resolution of a quarter degrees and 54 vertical layers. The runs consist of three parts: spin up procedure, numerical simulation in the North Pacific and numerical simulation over the regional domain (120-160°E, 10-50°N). The time step in MRI.COM was 10 minutes. The result of numerical simulation over the regional domain was used to investigate the processes of SSC production and to modify the entrainment parameterization (Deardorff, 1983) used in SOM.

The National Centre for Environmental Prediction (NCEP) Department of Energy Atmospheric Model Intercomparison Project reanalysis (hereafter, NCEP R-2) data was used as atmospheric forcing. However, wind stress was replaced with the objective analysis data in Japan Meteorological Agency merged with an artificial Rankin vortex based on Regional Specialized Meteorological Center (RSMC) tropical cyclone best-track data.

The detail of modification of the entrainment parameterization from the original Deardorff's scheme is in the followings:

**a.** Introduction of turbulent kinetic energy (TKE) production by wave breaking to turbulent transport term (add  $5u_*^3$  where  $u_*$  is the frictional velocity).

**b.** Relative contribution of an interfacial (gradient) Richardson number  $R_{iv}$  to an initial guess of turbulence Richardson number  $R_{iq}$  is reduced.

**c.** Proportional coefficient of third power of TKE ( $q_i^3$ ) in the turbulent dissipation term in the entrainment zone is changed from 0.07 to 1.0.

## 3. Results

### 3-1. Validity of simulated ocean response to Rex

Figure 1 illustrates the horizontal distribution of simulated sea temperature at a depth of 0.5 m (hereafter, SST in MRI.COM) and oceanic currents in case of the developing (Fig. 1a) and mature (Fig. 1b) stages with center positions of Rex denoted as typhoon symbols and observational points by R/V Keifu-Marui denoted as triangles. During the developing stage, moving speeds of Rex were relatively fast. In a fast translation, local SSC was significantly produced on the rightward of the moving direction.

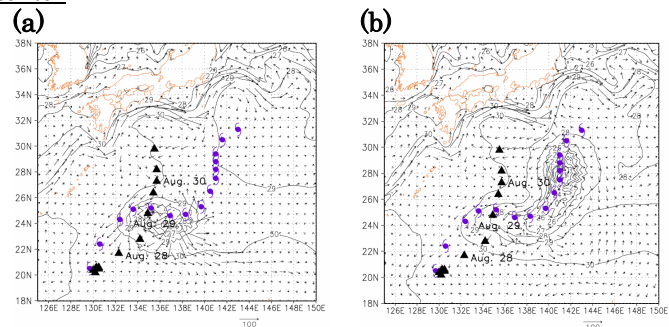


Fig.1 Horizontal distribution of simulated sea temperature at a depth of 0.5 m (contours), oceanic currents (vectors), center position of Rex (typhoon symbols), and observational points by R/V Keifu-Marui.

In contrast, local SSC was significantly produced around the center of Rex in a slow translation. Around the center, divergence was produced by Rex-induced currents. This reveals that upwelling was dominant around the area. The upwelling causes the increase in local SSC by Rex.

### 3-2. Relationship between TRMM/TMI three-day-mean SST and simulated SSTs

From the result of numerical simulation in MRI.COM, the relationship between TRMM/TMI three-day mean SST and simulated SSTs at the area with a  $6.25^\circ$  square centered at the Rex's center position (Fig. 2a) was investigated. The regression coefficient was nearly 0.99 and correlation coefficient was nearly 0.68. The high coefficients indicated that MRI.COM could properly reproduce SST. Figure 2b depicts the relationship between TRMM/TMI three-day mean SST and simulated SSTs in SOM at the same area. The positive bias of simulated SST was more obvious than the result in Fig. 2a. Figure 2c depicts the relationship between TRMM/TMI three-day mean SST and simulated SSTs in SOM with modified entrainment scheme (MSOM) at the same area. Both regression and correlation coefficients in MSOM were higher than those in SOM.

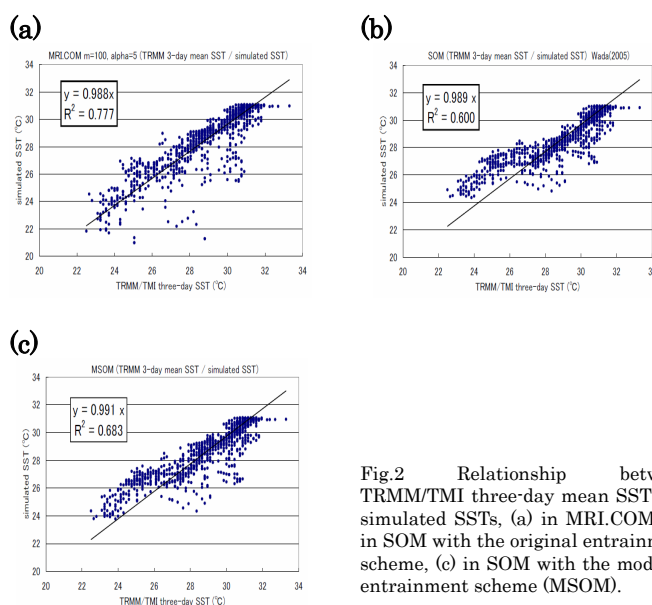


Fig.2 Relationship between TRMM/TMI three-day mean SST and simulated SSTs, (a) in MRI.COM, (b) in SOM with the original entrainment scheme, (c) in SOM with the modified entrainment scheme (MSOM).

### 3-3. Simulations of rapid SST decrease observed by R/V Keifu-Marui

Figure 3 depicts the time series of observed SST by R/V Keifu-Marui and simulated SSTs in each of ocean models: MRI.COM (Fig. 3a), SOM (Fig. 3a and 3b), and MSOM (Fig. 3b). Rapid decrease in SST, observed by R/V Keifu-Marui, was successfully simulated in MRI.COM, while the amplitude of decrease in SST in SOM was smaller than observational decrease in SST about  $3^\circ\text{C}$ , which was in contrast to the result of Wada (2005). The relatively low amplitude of SST decrease was partly because atmospheric forcing used in the present investigation was different from that in Wada (2005). The MSOM could successfully simulate the rapid decrease in SST.

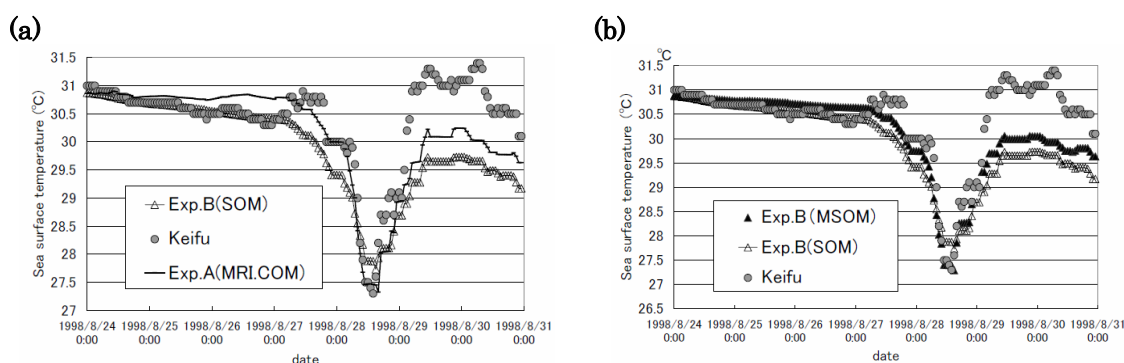


Fig.3 Time series of SST observed by R/V Keifu-Marui and simulated SST at the same locations. (a) Observed SST and simulated SSTs in MRI.COM and SOM with the original entrainment scheme. (b) Observed SST and simulated SSTs in SOM and MSOM.

### References

- Deardorff, J. W. (1983): A multi-limit mixed-layer entrainment formulation. *J. Phys. Oceanogr.*, **13**, 988-1002.
- Ishikawa, I., et al. (2005): Meteorological Research Institute Community Ocean Model (MRI.COM) manual. *Technical Reports of the Meteorological Research Institute*, **47**, 189pp. (in Japanese).
- Wada, A. (2005): Numerical simulations of sea surface cooling by a mixed layer model during the passage of Typhoon Rex. *J. Oceanogr.* **61**, 41-57.

# Interannual Variations of the Upper Ocean Mixed Layer in Deep Convection Regions as Revealed by Numerical Experiments With an OGCM

Alexander A. Zelenko and Yurii D. Resnyansky

Hydrometeorological Research Center of Russian Federation,  
Bol. Predtechensky per., 11-13, 123242 Moscow, Russia E-mail: [zelenko@mecom.ru](mailto:zelenko@mecom.ru)

Variations of the upper ocean mixed layer depth reflect the processes of sea-air interaction and of intrinsic ocean dynamics in a broad range of spatial and time scales. The most vigorous mixing is induced by density convection during the cold season within spatially restricted regions. In modern climatic conditions, the main regions of open ocean deep convection are situated in the Greenland and Labrador Seas (Marshall and Schott, 1999). Available, rather sparse, observational data indicate violent interannual variability of convective mixing intensity in such regions (e.g. Lab Sea Group, 1998).

Numerical experiments have been performed with an OGCM (Resnyansky and Zelenko, 1999) in order to elucidate the mechanisms liable for interannual variations of the upper ocean mixed layer depth (MLD) in deep convection regions. The vertical turbulent mixing in the upper ocean layer induced by wind stirring and by surface buoyancy flux is described in the OGCM using the concept of bulk mixed layer model with potential temperature, salinity, and water density distributions a priori homogeneous in the vertical. The algorithm of convective adjustment was used to parameterize the density convection, which may develop not only in the near-surface layer, but also at any depth. This algorithm ensures the complete elimination of unstable parts of a density profile at each time step. It is similar to that of (Rahmstorf, 1993), accepted as a primary option of convective adjustment in last versions of the MOM ocean model.

The computations have been performed using the 6-hourly data on atmospheric forcing, which enable to monitor the variability at time scales from several days to several years.

Figure 1 shows temporal changes of MLD averaged over the Labrador (46°-64°N, 40°-60°W) and Greenland (67°-80°N, 25°W-20°E) regions during 1987–2002. The interannual variability reveals itself in changes of the MLD seasonal maximum and in the strength of fluctuations at time scales of 5–10 days. A number of observational evidence can be found for variations of the MLD seasonal maximum (of an order of 1000 m for the Labrador Sea) obtained in the model. Thus, according to (Lab Sea Group, 1998), the 1993 winter in the Labrador Sea has been marked by extremely strong convective activity with mixing depths more than 2200 m. However, during subsequent winters, the convection was much weaker, and in the 1995/1996 winter, MLD didn't exceed 1000 m. Such variations (Lab Sea Group, 1998) can be related to the North Atlantic Oscillation, the most important signal of interannual variability in the North Atlantic. They are satisfactorily reproduced (Fig. 1) in the numerical experiment. The main model tendencies of interannual variability are also confirmed by some other observations (Lavender et al., 2002; Pickart et al., 2002; Schott et al., 1993).

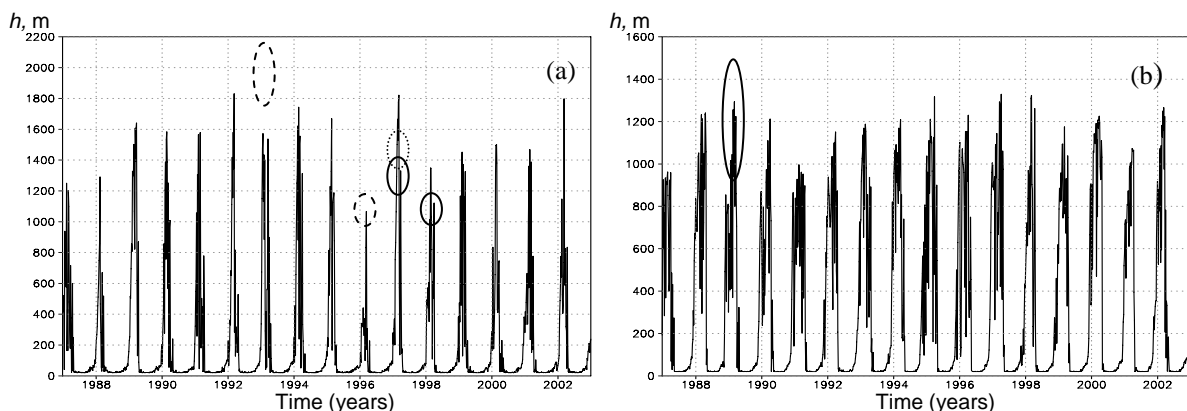


Fig. 1. Temporal changes of computed MLD ( $h$ , m) averaged over the Labrador (a) and Greenland (b) regions. Ovals with different edging show the ranges of convective mixing depths according to observational evidences (Lab Sea Group, 1998 – dashed), (Lavender et al., 2002 – solid), (Pickart et al., 2002 – dotted) over the Labrador Sea, and (Schott et al., 1993 – solid) over the Greenland Sea.

To reveal the role of different factors in variations of MLD ( $h$ ), we compared the time series of  $h$  and the determining factors. Figure 2 shows the interannual changes of mean values of  $h$  together with buoyancy flux  $B_0$ , vertical component of current velocity curl  $rot \mathbf{u}$ , and vertical component of current speed  $w$  itself at 500-m depth.

A rather clear interrelation is seen between the changes of  $h$  and  $B_0$ . An increase (decrease) in buoyancy loss is most often accompanied by an MLD increase (decrease). The absolute maximum of  $h$  in 1989 contemporize

with  $|B_0|$  maximum. However, in some cases, the tendencies in changes of  $h$  from one year to another are not consistent with the tendencies in changes of buoyancy flux. For example, buoyancy loss noticeably decreased from 1991 to 1992, whereas MLD didn't change or even slightly increased. The similar situation is found for 1998/1999, 1999/2000, and 2001/2002 winters.

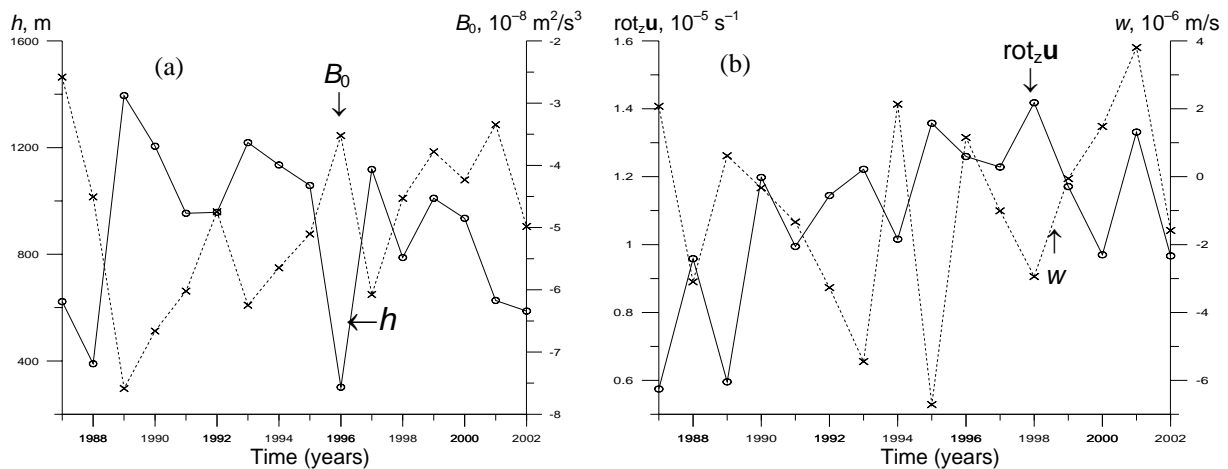


Fig. 2. Interannual variability of model seasonal mean of convective mixing depth and of associated variables in the Labrador region ( $55^{\circ}$ – $42^{\circ}$ W,  $53^{\circ}$ – $59^{\circ}$ N). (a) – January–March mean MLD  $h$  (left scale, m) and the surface buoyancy flux  $B_0$  (right scale,  $10^{-8} \text{ m}^2/\text{s}^3$ ); (b) – December mean dynamical characteristics at 500-m depth: vertical component of ocean current velocity curl  $\text{rot}_z \mathbf{u}$  (left scale,  $10^{-5} \text{ s}^{-1}$ ), and vertical component of current speed itself  $w$  (right scale,  $10^{-6} \text{ m/s}$ ). Positive  $w$  corresponds to descending motions.

Dynamical factors can cause discrepancies between  $h$  and  $B_0$  in these years. As is well known (e.g. Marshall and Schott, 1999), an enhancement of cyclonic circulation in the ocean prior to strong cooling of its surface results in raising of underlying weekly stratified waters nearer to the surface, and this, in turn, fosters the penetration of convective mixing to greater depths. Taking into account this fact allows one to advance in explaining indicated above peculiarities in Fig. 2. Thus, with reference to 1991/1992 it may be seen that enhanced cyclonicity of the circulation in 1992 favored the maintenance of deeper mixing even against the background of weakened surface buoyancy loss. The processes during 2001/2002 winter may be interpreted in a similar way.

The explanation for convective seasons in 1999 and 2000, when deeper mixed layer was observed during weakened buoyancy flux and concurrent decrease of  $\text{rot}_z \mathbf{u}$ , can be related to immediate influence of vertical motions. As is seen from Fig. 2b, the vertical velocity  $w$  at 500 m depth prior to the beginning of these convective periods was close to zero (in 1999) or positive (in 2000). That is, a large scale sinking took place at this time instead of an ascent, which, presumably, influenced the development of convective processes.

Taking into account the ocean state before the beginning of convective season also enables us to clarify the noticeable differences in mean MLD during different years with approximately identical buoyancy fluxes. Thus, in 1992 and 2002, the mean buoyancy loss from the ocean surface was about  $-5 \times 10^{-8} \text{ m}^2/\text{s}^3$ , whereas MLD differed by a factor of one and a half. The difference can be caused by different  $\text{rot}_z \mathbf{u}$  and  $w$  before convective seasons during these years.

## REFERENCES

- Lab Sea Group, 1998: The Labrador Sea Deep Convection Experiment. *Bull. Amer. Meteorol. Soc.*, **79**, 2033–2058.
- Lavender, K.L., R. E. Davis, and W.B. Owens, 2002: Observations of open-ocean deep convection in the Labrador Sea from subsurface floats. *J. Physical Oceanogr.*, **32**, 511–526.
- Marshall, J., and F. Schott, 1999: Open-ocean convection: Observations, theory, and models. *Rev. Geophys.*, **37**, 1–64.
- Pickart, R.S., D.J. Terres, and R.A. Clarke, 2002: Hydrography of the Labrador Sea during active convection. *J. Phys. Oceanogr.*, **32**, 428–457.
- Rahmstorf, S., 1993: A fast and complete convection scheme for ocean models. *Ocean Modelling*, **101**, 9–11.
- Resnyansky, Yu.D., and A.A. Zelenko, 1999: Effects of synoptic variations of atmospheric forcing in an ocean general circulation model: Direct and indirect manifestations. *Russian Meteorology and Hydrology*, **9**, 42–50.
- Schott, F., M. Visbeck, and J. Fischer, 1993: Observations of vertical currents and convection in the central Greenland Sea during the winter of 1988/1989. *J. Geophys. Res.*, **C98**, 14401–14421.